stellar systems

Large N systems interacting with long-range forces

$$F = G M m / r^2$$

planetary system;
galactic nucleus star cluster;
globular cluster;
galaxy;
cluster of galaxy…

First classification: collisional vs. collisionless

stars are in general collision-less;
galaxies may not be.

Collisionless separated into: relaxed vs. unrelaxed
(sometimes confusingly called 'collisional vs. collisionless')

un-relaxed system preserves initial memory,
— tidal stream, halo star,…

while relaxed system don't. They are thermalized.
— globular cluster;
— group/cluster of galaxies;

relaxation processes:
2-body relaxation, violent relaxation…

First consider a test particle's motion in 'smooth' potentials

spherical potentials

potential-density pair
circular motion
non-circular motion & precession

BT 2.2, 3.1

point mass (Keplerian)

uniform sphere

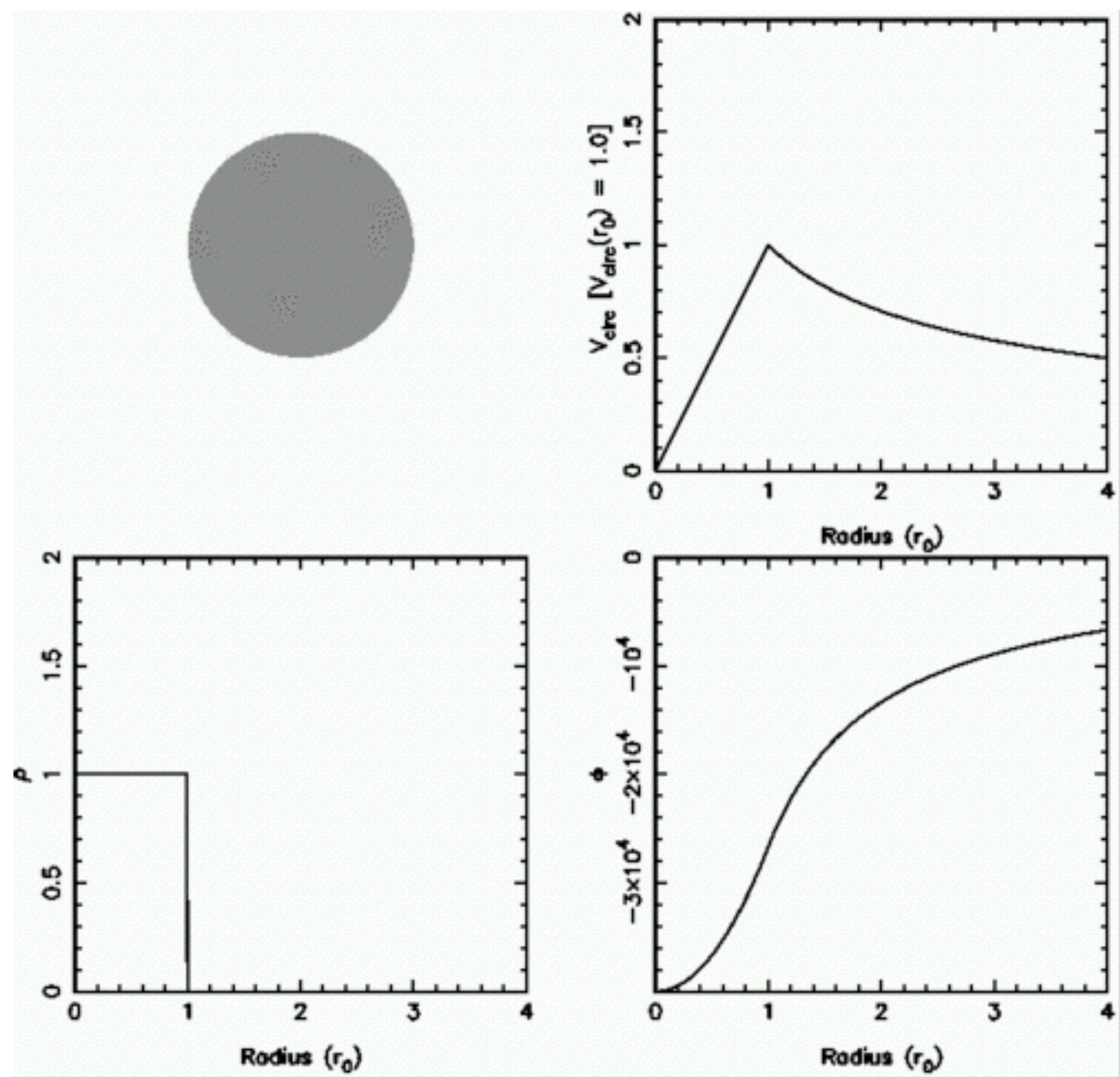

Plummer potential

is analytic solution of hydrostatic support for polytropic stellar system of index 5;

(r) matches GCs well, but is too steep at large r for Ellipticals (r^{-5}).

$$\rho_P(r) = \left(\frac{3M}{4\pi b^3}\right)\left(1+\frac{r^2}{b^2}\right)^{-5/2} \quad ; \quad \Phi_P(r) = -\frac{GM}{\sqrt{r^2+b^2}}$$

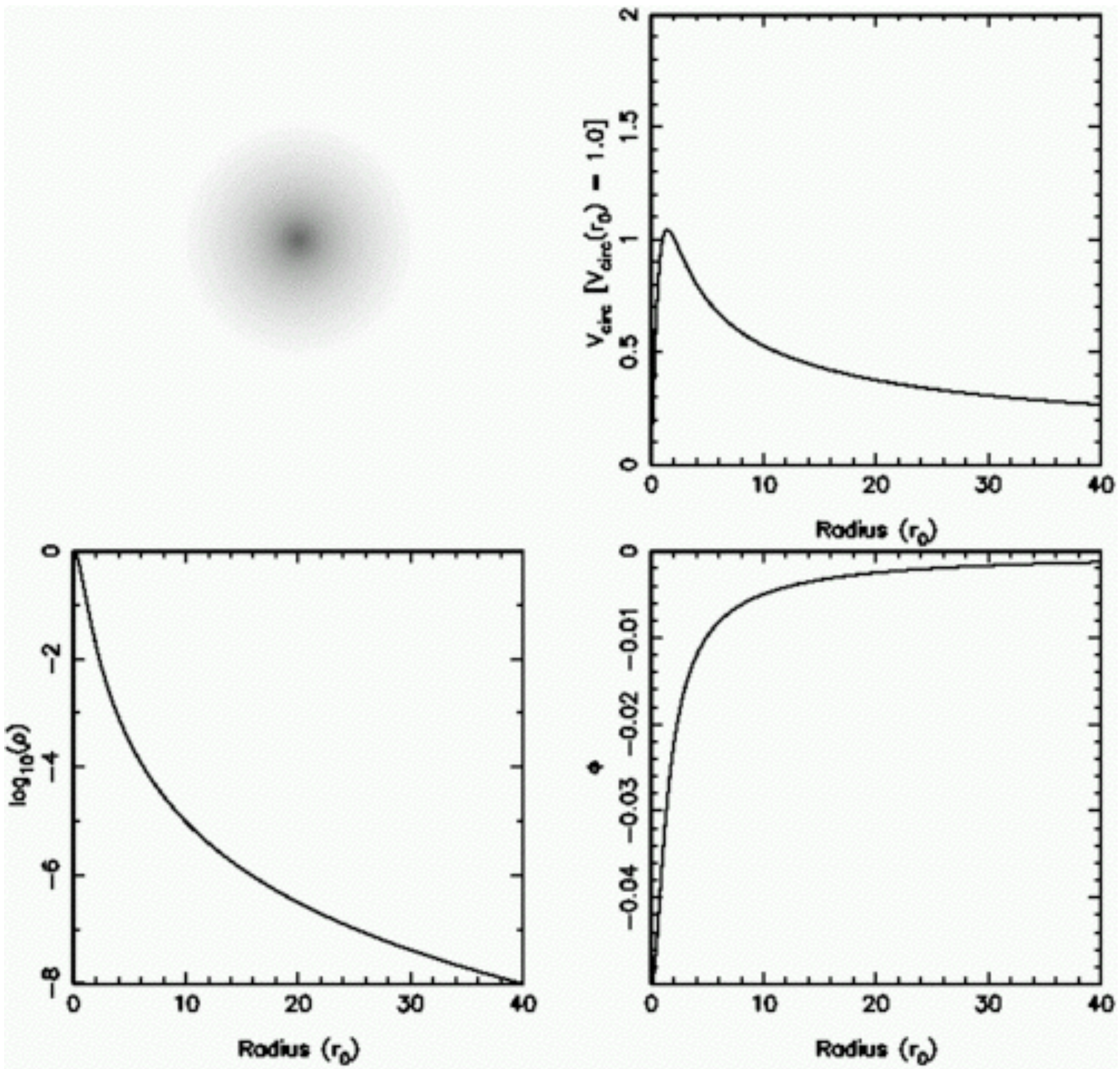

isothermal sphere

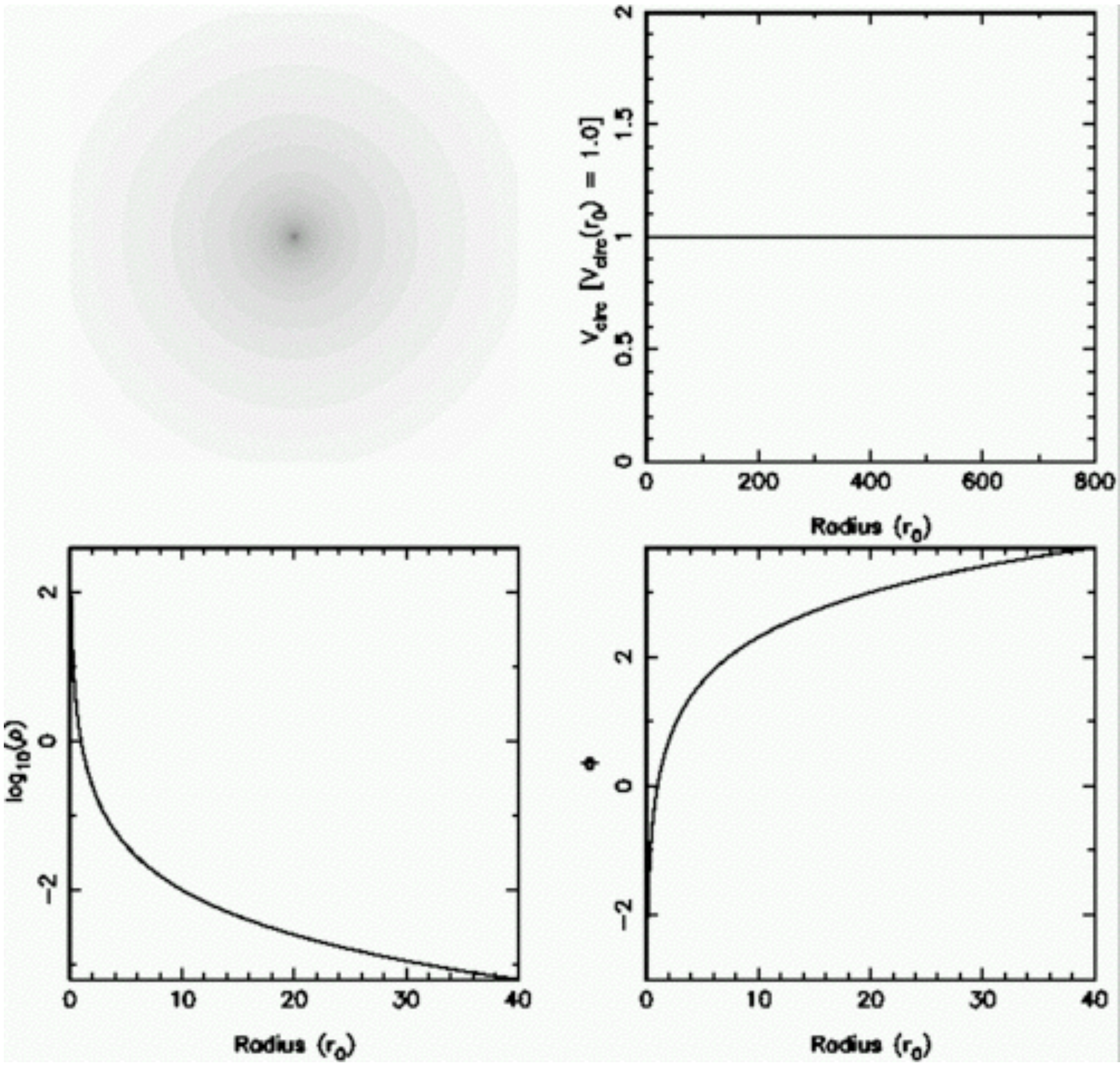

NFW (Navarro, Frenk & White '95) for dark matter halos

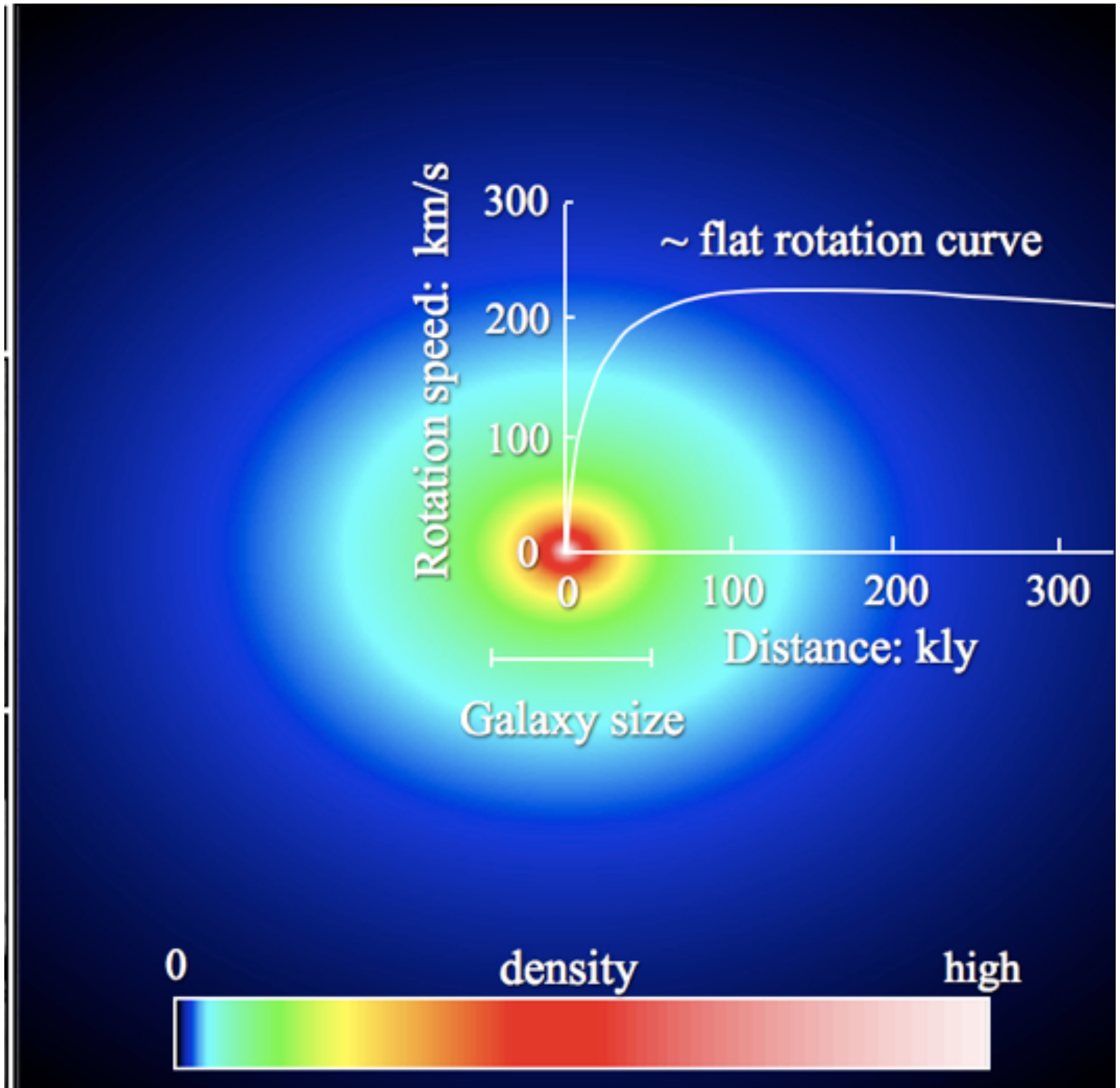

$$\rho(r) = \frac{\rho_0}{(r/a)(1+r/a)^2}$$

The density of a NFW dark matter halo is shown color coded, along with its circular rotation curve.

This results from fits to n-body codes that follow the cosmological evolution of dark matter, and its hierarchical merging to form dark matter halos. Perhaps surprisingly, no matter what the size of the halo, roughly the same universal density law arises, from dwarf galaxy mass, through galaxy mass, to cluster mass.

Although the rotation curves ultimately decline, they appear flat over a large region which is sampled by the HI disks

Two-power density models

$$\rho(r) = \frac{\rho_0}{(r/a)^\alpha (1 + r/a)^{\beta-\alpha}}.$$

$$\Phi = -G \int_r^\infty \mathrm{d}r \, \frac{M(r)}{r^2}$$
$$= -4\pi G \rho_0 a^2 \times \begin{cases} \ln(1 + a/r) & \text{for a Jaffe model} \\ \dfrac{1}{2(1 + r/a)} & \text{for a Hernquist model} \\ \dfrac{\ln(1 + r/a)}{r/a} & \text{for a NFW model.} \end{cases}$$

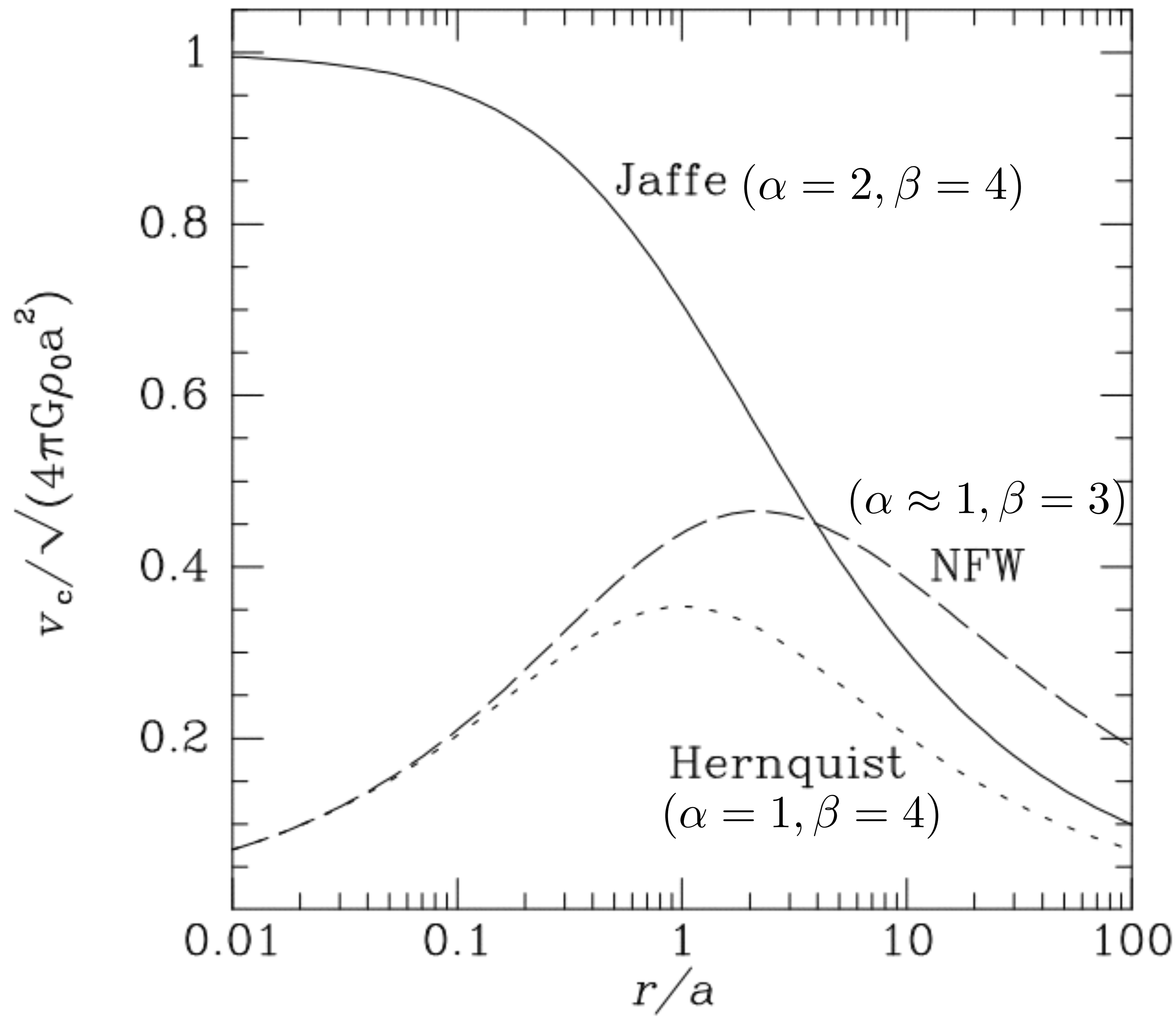

NFW ('96) showed that larger halos are more massive, a scales with R_{200}

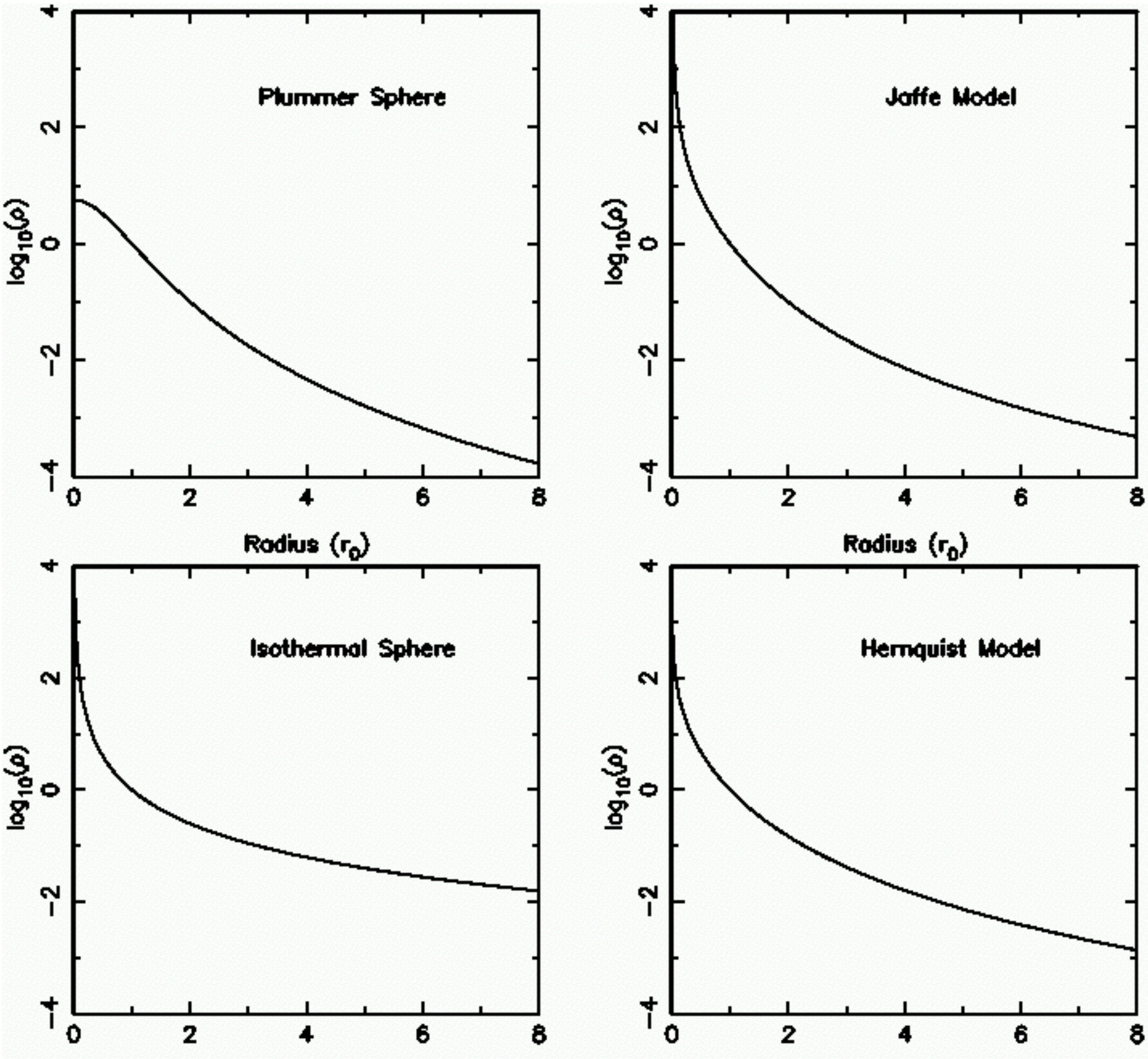
Plummer Sphere
Jaffe Model
Isothermal Sphere
Hernquist Model
$\log_{10}(\rho)$
Radius (r_0)
4
2
0
-2
-4
0
2
4
6
8

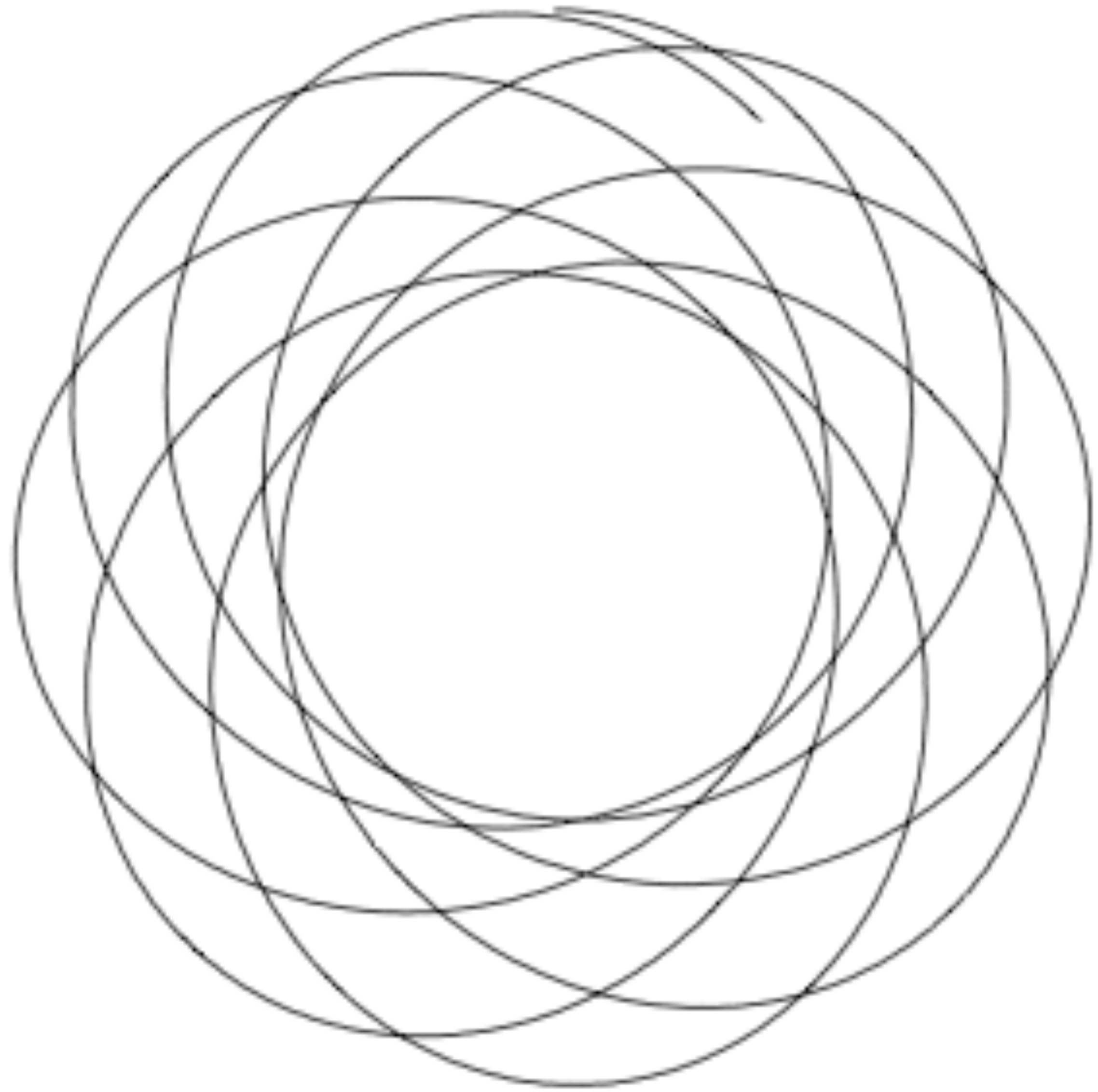

Figure 3.1 A typical orbit in a spherical potential (the isochrone, eq. 2.47) forms a rosette.

Orbits in a spherical potential stay in a plane.

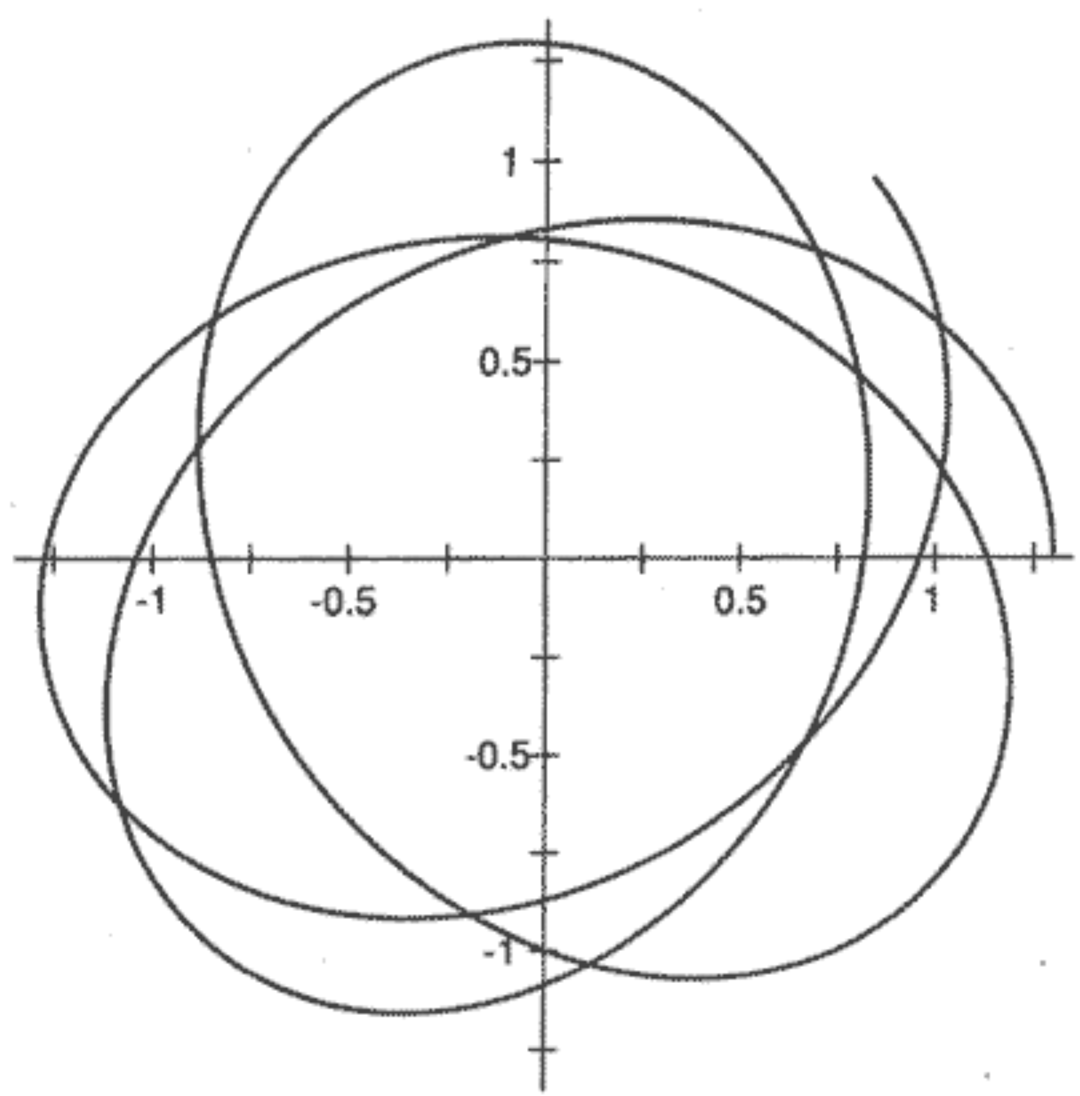

Figure 3.9 Path of the star of Figure 3.7, viewed from above the Galactic plane; the orbit started with ($R = 1.3,\ \phi = 0$) and ($\dot{R} = 0,\ R\dot{\phi} = 0.4574$).

Non-spherical potential:
axisymmetric

$$\Phi = \Phi(R, z)$$

homoeoid
circular motion
non-circular motion & precession

BT 2.3, 3.2

orbits are not simple Keplerian ellipses

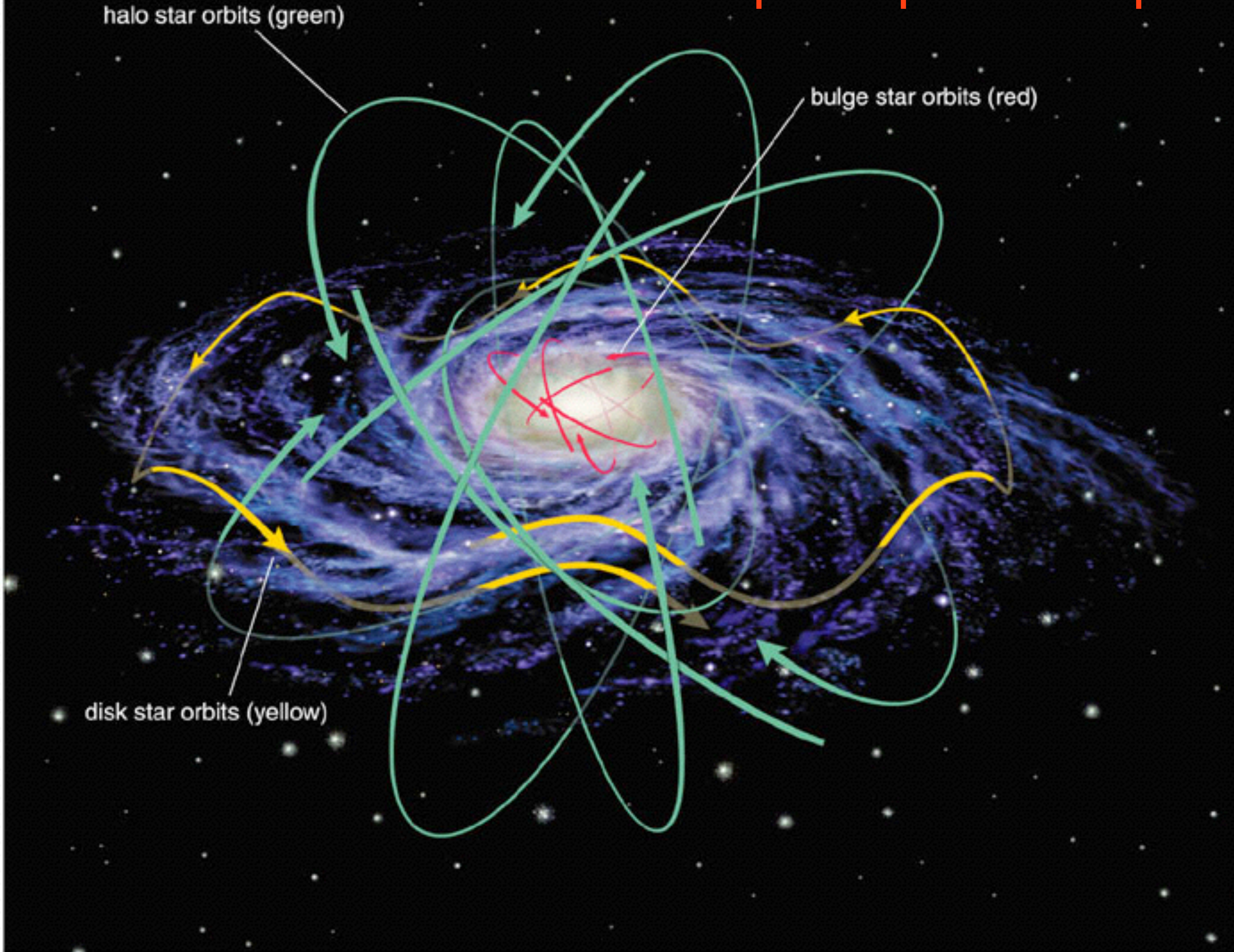

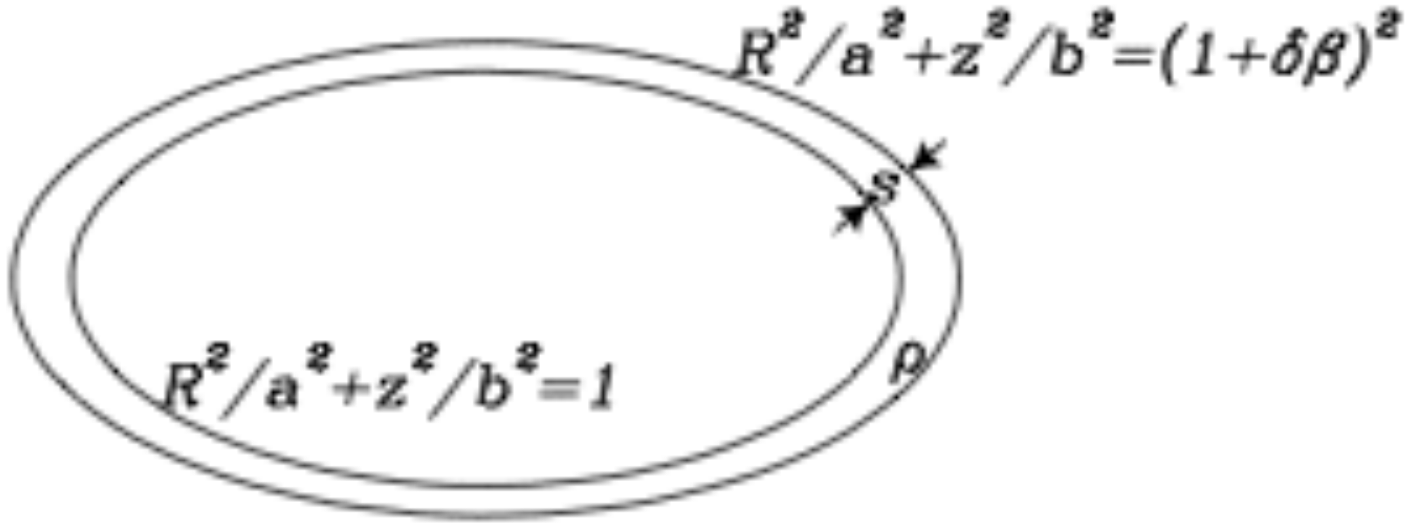

Figure 2.12 A homoeoid of density ρ is bounded by the surfaces $R^2/a^2 + z^2/b^2 = 1$ and $R^2/a^2 + z^2/b^2 = (1 + \delta\beta)^2$. The perpendicular distance s between the bounding surfaces varies with position around the homoeoid.

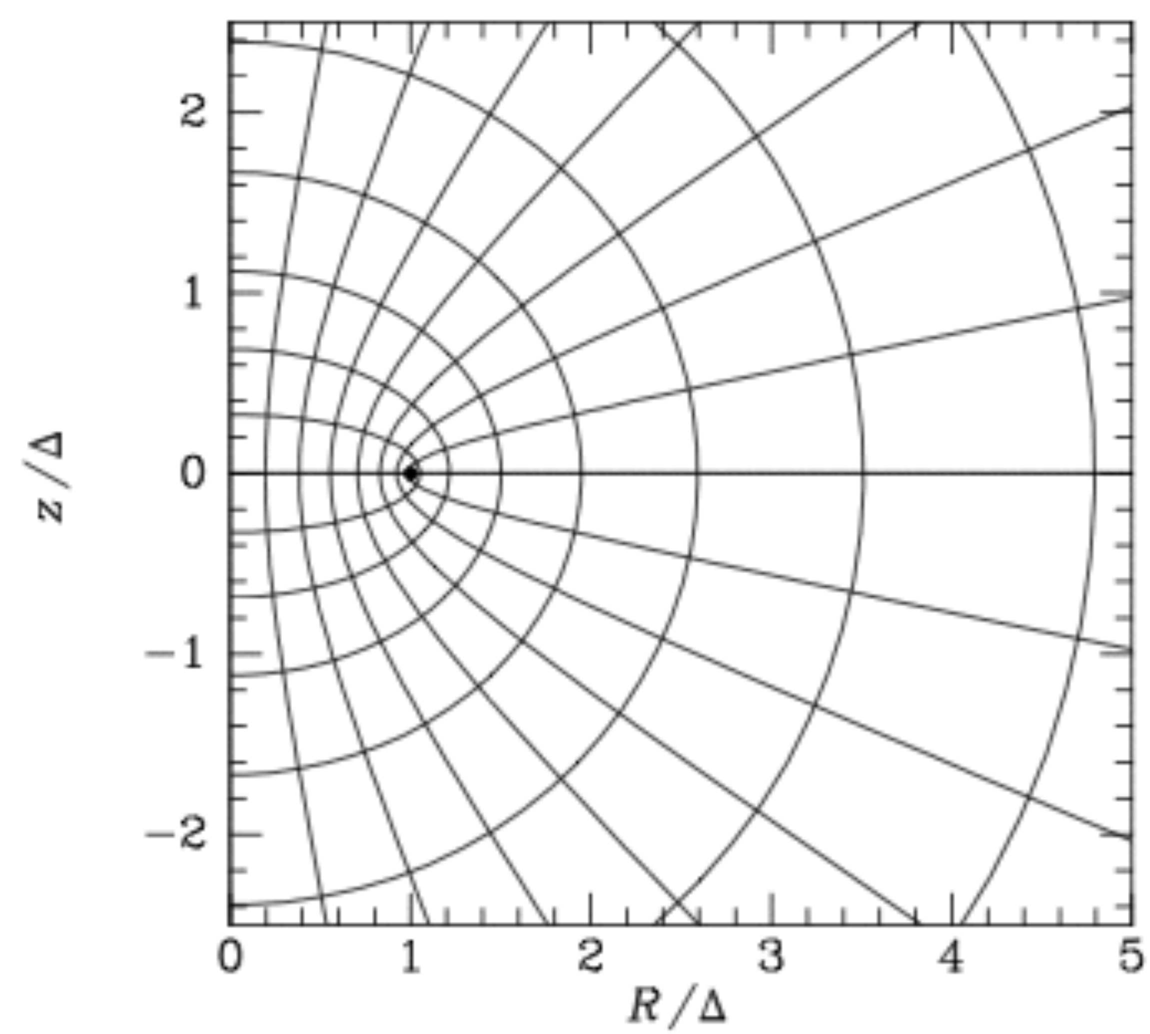

Figure 2.11 Curves of constant u and v in the (R, z) plane. Semi-ellipses are curves of constant u, and hyperbolae are curves of constant v. The common focus of all curves is marked by a dot. In order to ensure that each point has a unique v-coordinate, we exclude the disk $(z = 0,\ R \leq \Delta)$ from the space to be considered.

for a thin-disk

mid-plane circular velocity

$$v_c^2(R) = R\, \frac{\partial \Phi(R,z)}{\partial R}\bigg|_{z=0}$$

What if one writes:

$$v_c^2(R) = \frac{GM(<R)}{R}?$$

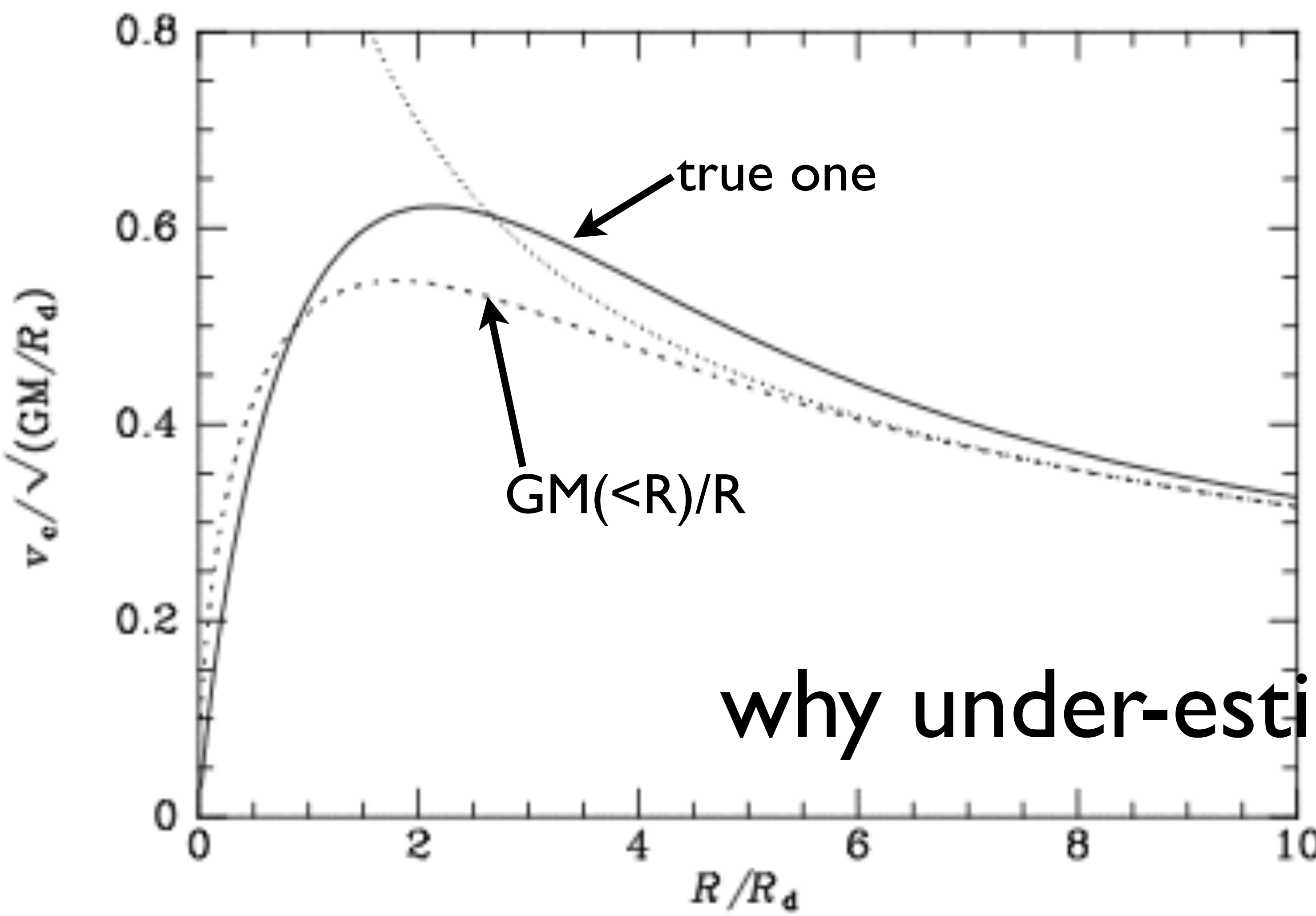

why under-estimate velocity?

Figure 2.17 The circular-speed curves of: an exponential disk (full curve); a point with the same total mass (dotted curve); the spherical body for which $M(r)$ is given by equation (2.166) (dashed curve).

why under-estimate velocity?

all rings contribute

$$v_c^2(R) = R\frac{\partial \Phi}{\partial R} = -4G\int_0^R \mathrm{d}a\,\frac{a}{\sqrt{R^2-a^2}}\frac{\mathrm{d}}{\mathrm{d}a}\int_a^\infty \mathrm{d}R'\,\frac{R'\Sigma(R')}{\sqrt{R'^2-a^2}}. \quad (2.157)$$

individual ring: all homoeoids with a > R contributes

$$\Sigma(R) = \sum_{a\geq R}\delta\Sigma(a,R) = \int_R^\infty \mathrm{d}a\,\frac{\Sigma_0(a)}{\sqrt{a^2-R^2}}. \quad (2.148a)$$

However, one is still allowed to (and indeed one does) write $v_c^2(R) \approx \frac{GM(<R)}{R}$

logarithmic potential (spheroidal)

$$\Phi_{\rm eff} = \tfrac{1}{2}v_0^2 \ln\left(R^2 + \frac{z^2}{q^2}\right) + \frac{L_z^2}{2R^2}, \qquad (3.70)$$

guiding centre: minimum in $\Phi_{\rm eff}$.

$$\frac{\partial\Phi_{\rm eff}}{\partial R} = 0$$

$$\frac{\partial\Phi_{\rm eff}}{\partial z} = 0$$

steep potential wall; Lz conservation means all orbits avoid center

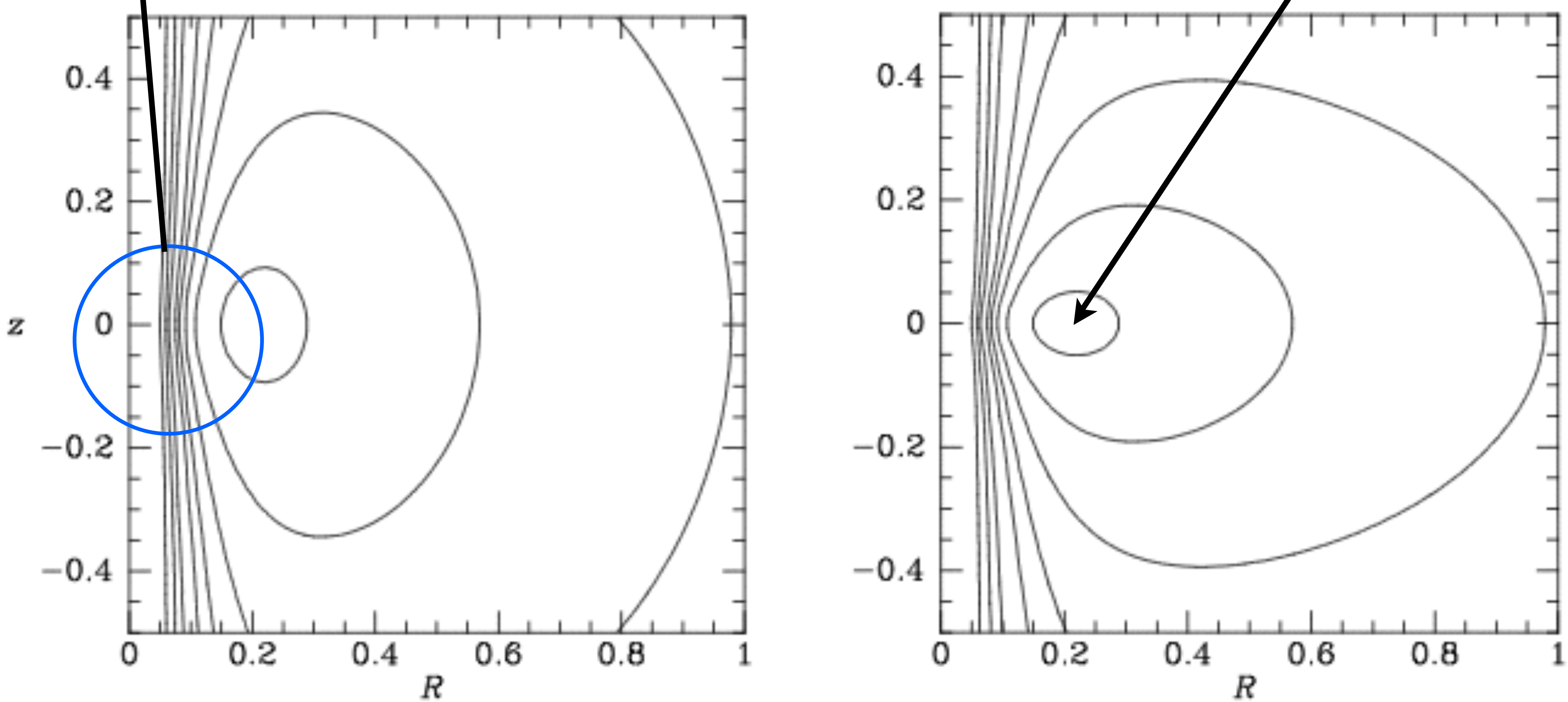

Figure 3.3 Level contours of the effective potential of equation (3.70) when $v_0 = 1$, $L_z = 0.2$. Contours are shown for $\Phi_{\rm eff} = -1, -0.5, 0, 0.5, 1, 1.5, 2, 3, 5$. The axis ratio is $q = 0.9$ in the left panel and $q = 0.5$ in the right.

different zvc for orbits of different energy

3D motion --> (E/Lz conservation) ---> 2D motion

different orbits even with the same E/L_z

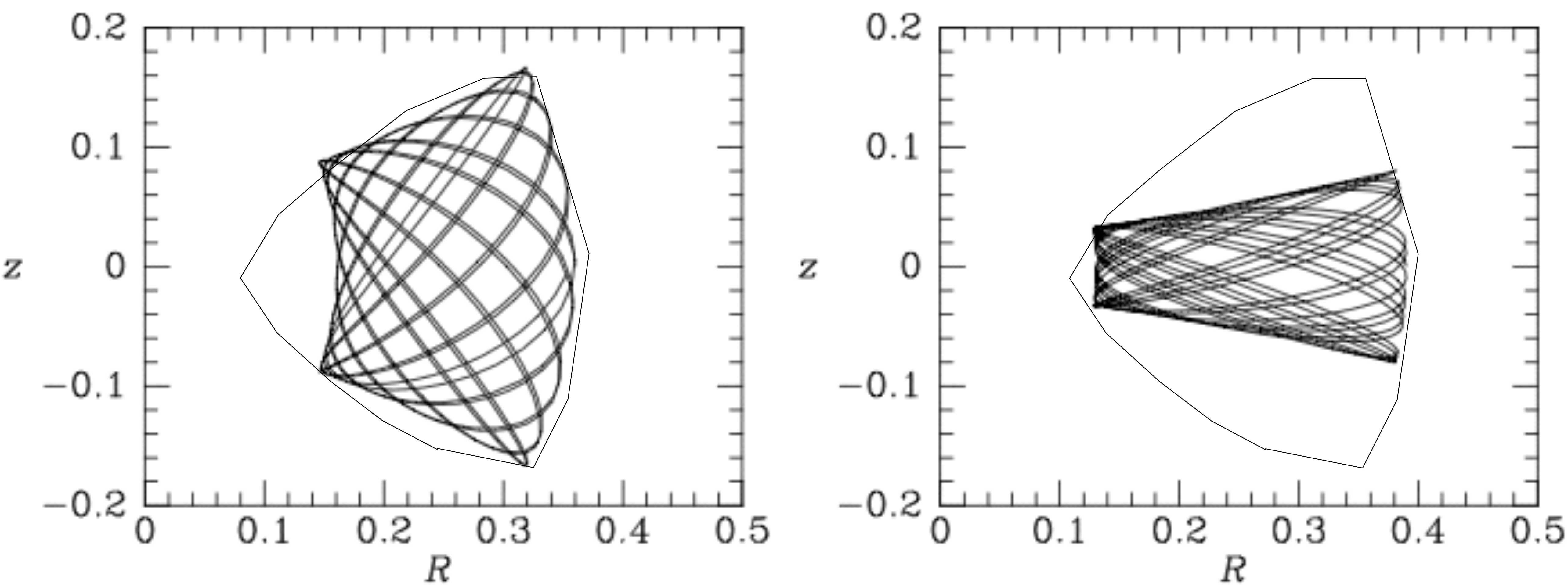

Figure 3.4 Two orbits in the potential of equation (3.70) with $q = 0.9$. Both orbits are at energy $E = -0.8$ and angular momentum $L_z = 0.2$, and we assume $v_0 = 1$.

. gradual precession of the orbital plane
. space allowed by ZVC not filled up -- 3rd integral

graphing the orbit:

3-D ----> 2-D ----> 1-D

strobe (**surface of section**)

e.g., when $z=0$, $p_z > 0$

Jules Henri Poincaré (1854–1912). Photograph from the frontispiece of the 1913 edition of *Last Thoughts*.

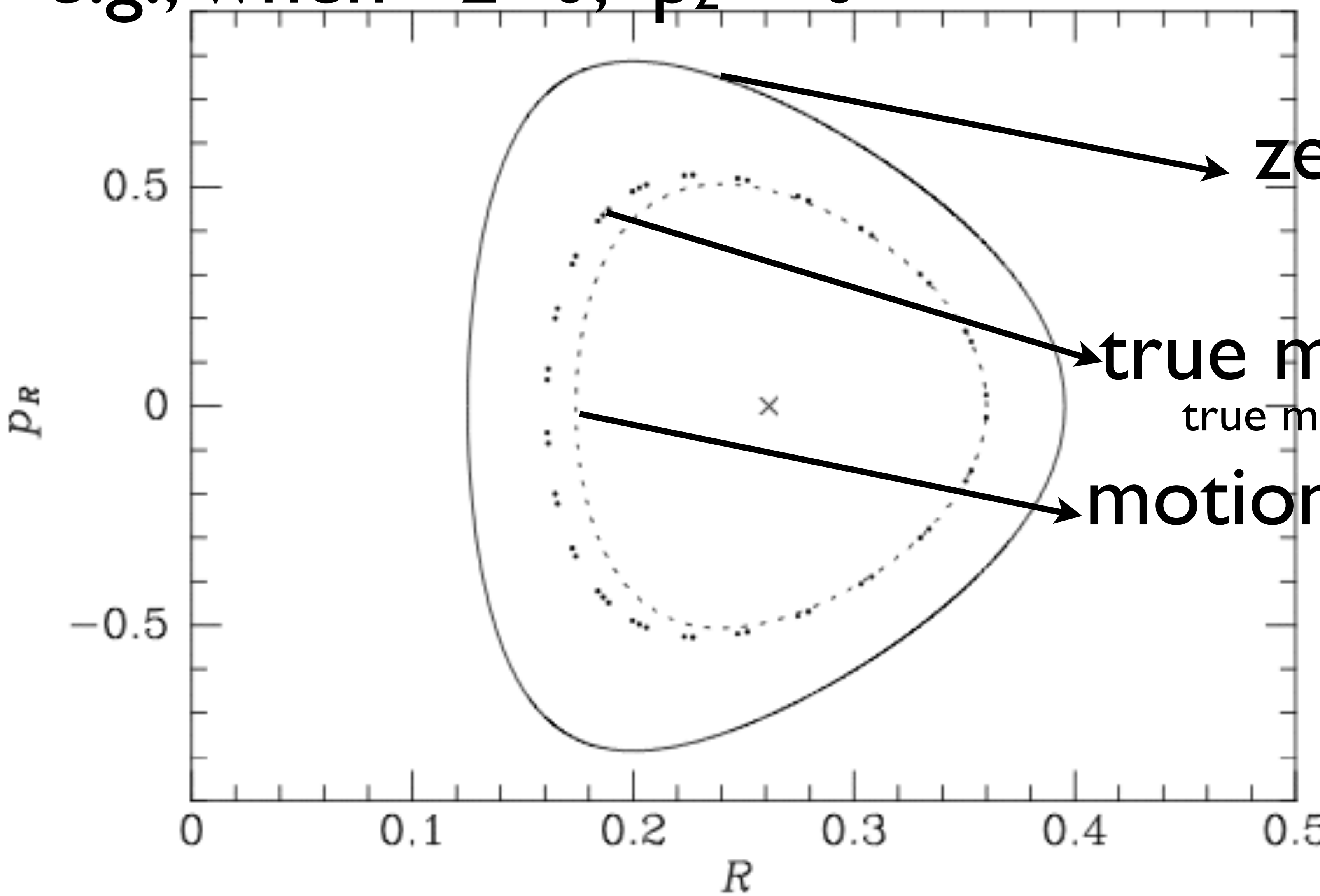

re **3.5** Points generated by the orbit of the left panel of Figure 3.4 in the (R, p_R) ce of section. If the total angular momentum L of the orbit were conserved, the points d fall on the dashed curve. The full curve is the zero-velocity curve at the energy of orbit. The × marks the consequent of the shell orbit.

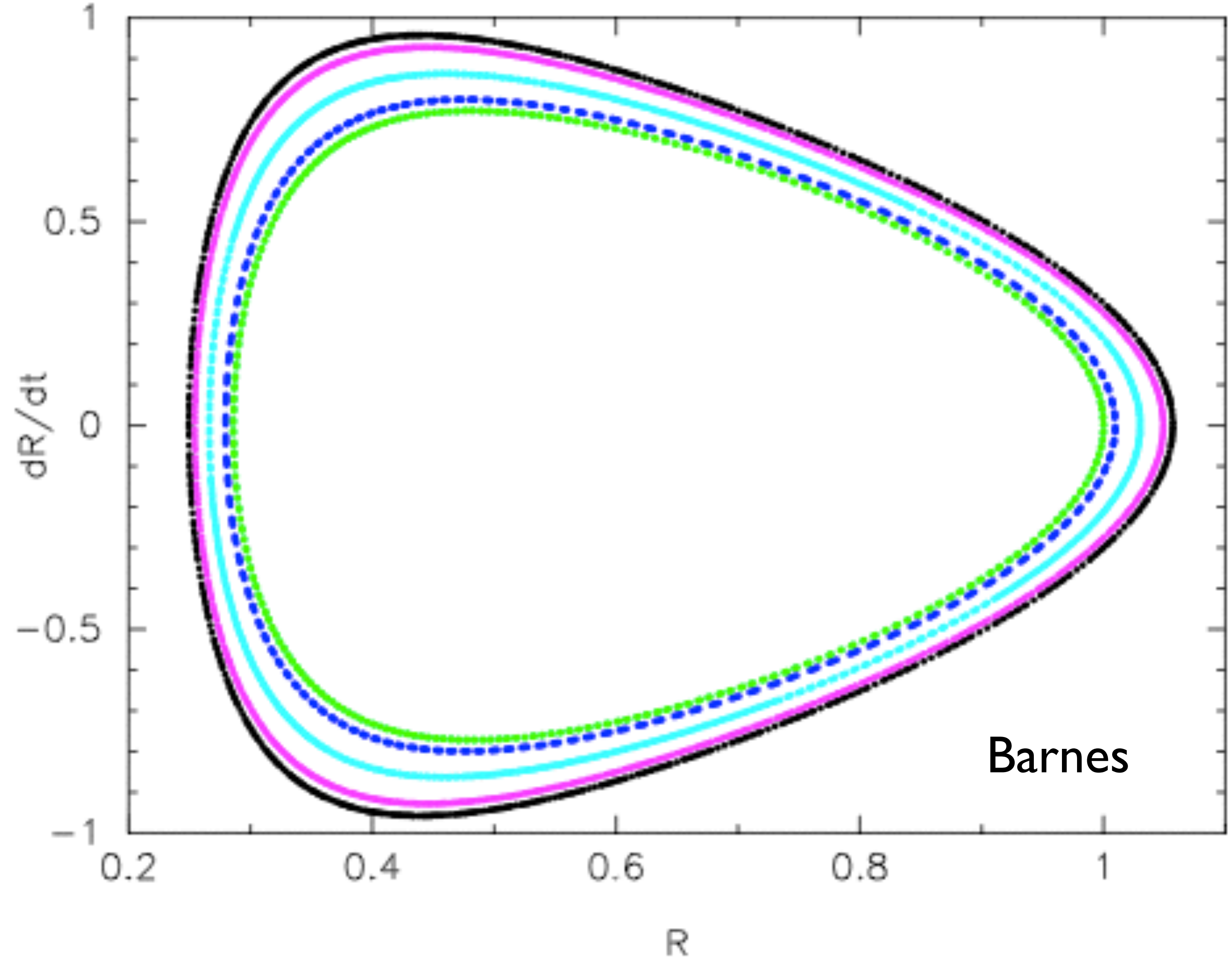

Figure 8.2: Surface of section for five orbits in the logarithmic potential (8.1

total L almost conserved

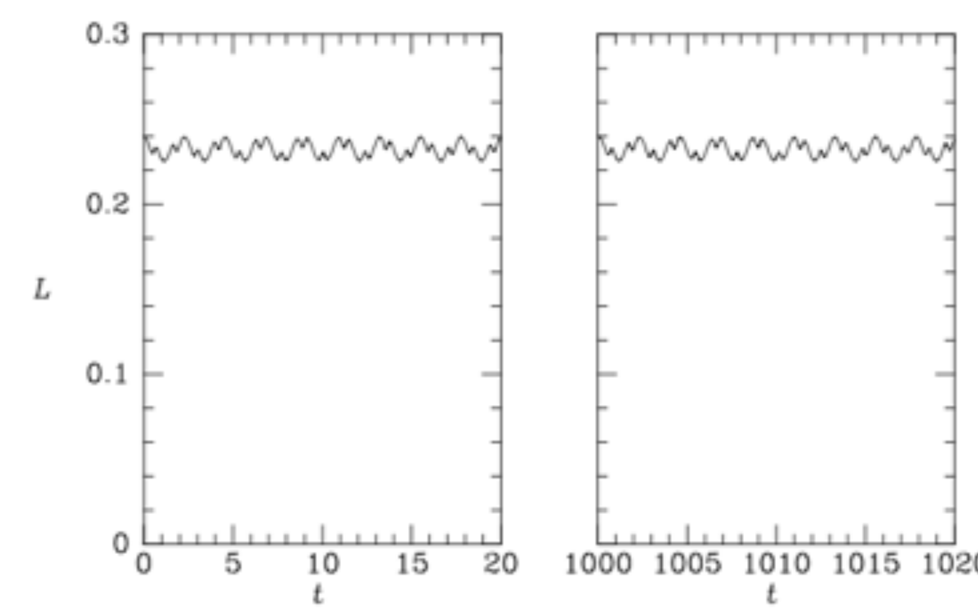

Figure 3.6 The total angular momentum is almost constant along the orbit shown in th
left panel of Figure 3.5. For clarity $L(t)$ is plotted only at the beginning and end of a lon
integration.

same E/L_z

non-crossing in surface of section

bound by a 3rd integral

Surface of section of Pluto's moon, Nix

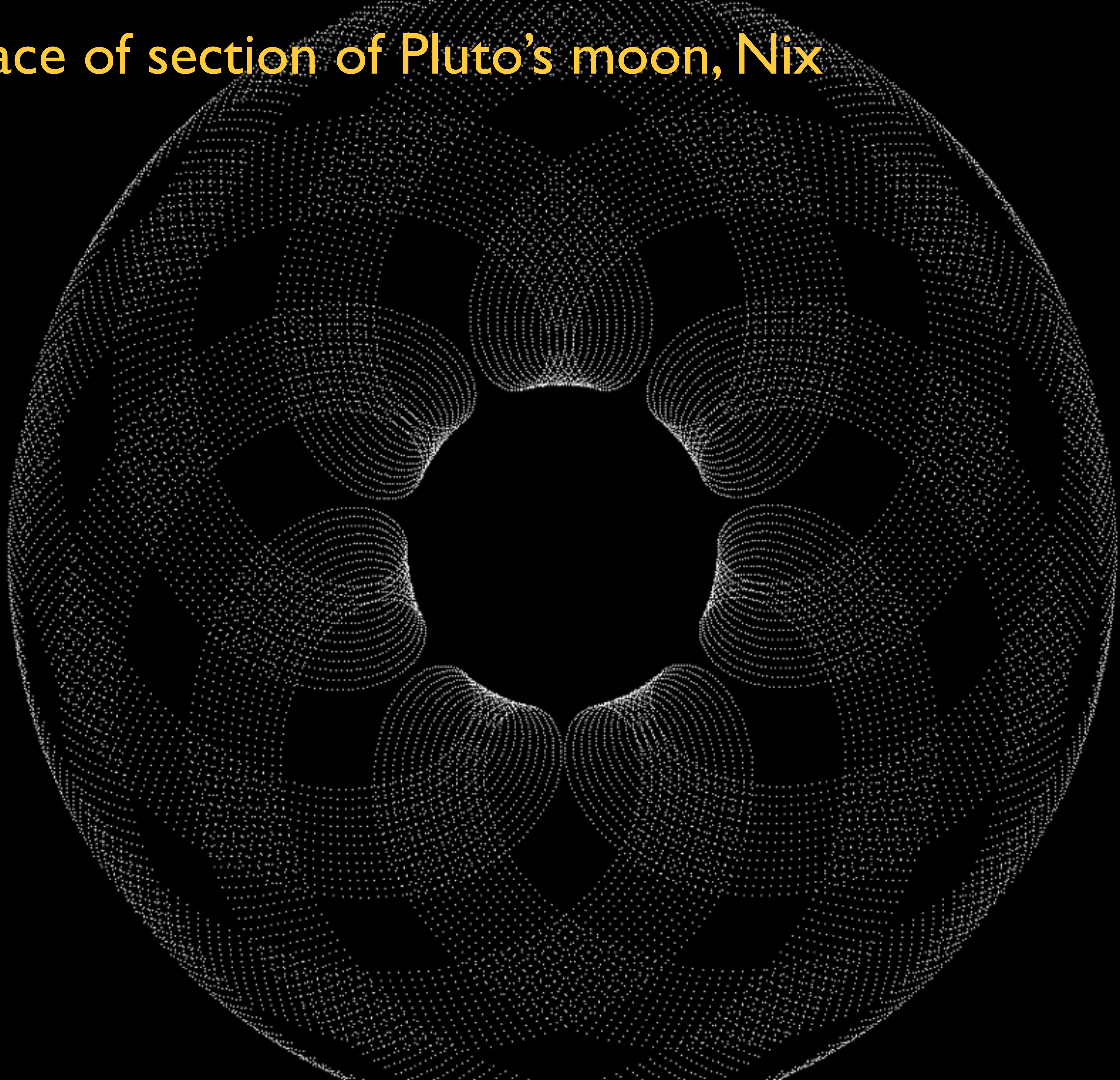

Surface of section depends on: potential form; E, L_z

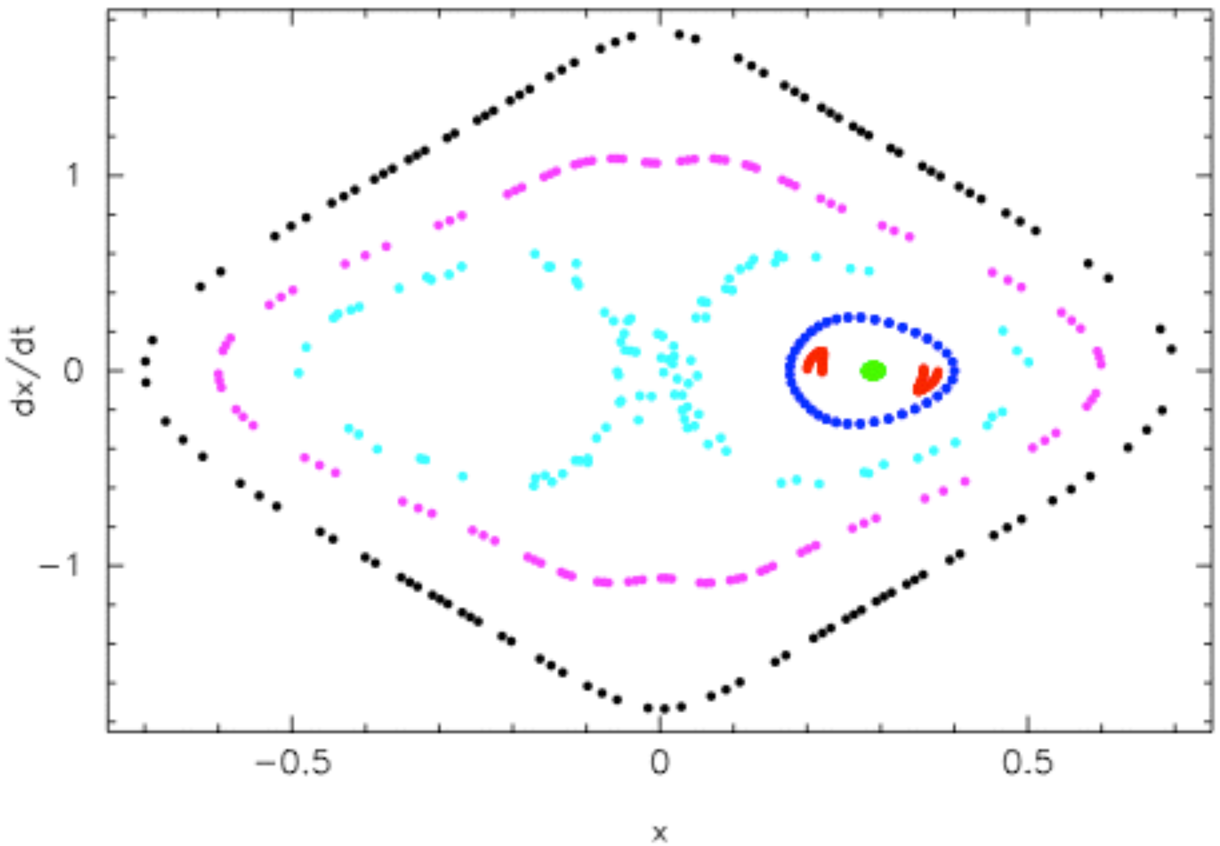

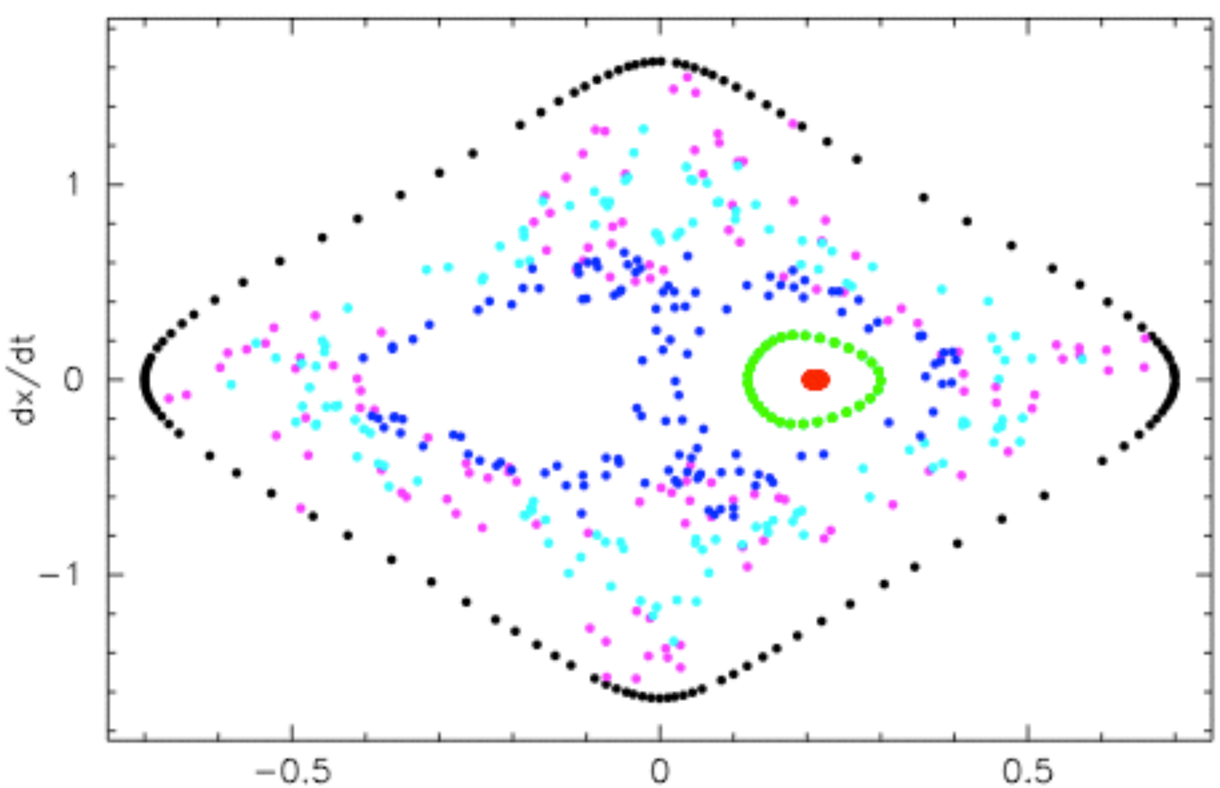

regular orbits: 3 integrals of motion

chaotic orbits: too few integrals, motion “ergodic”

resonant orbits: special regular orbits with commensurable frequencies

$$\Phi_{\rm eff} = \Phi_{\rm eff}(R_{\rm g},0) + \tfrac{1}{2}\left(\frac{\partial^2\Phi_{\rm eff}}{\partial R^2}\right)_{(R_{\rm g},0)} x^2 + \tfrac{1}{2}\left(\frac{\partial^2\Phi_{\rm eff}}{\partial z^2}\right)_{(R_{\rm g},0)} z^2 + {\rm O}(xz^2). \quad (3.76)$$

$$\kappa^2(R_{\rm g}) \equiv \left(\frac{\partial^2\Phi_{\rm eff}}{\partial R^2}\right)_{(R_{\rm g},0)} \quad ; \quad \nu^2(R_{\rm g}) \equiv \left(\frac{\partial^2\Phi_{\rm eff}}{\partial z^2}\right)_{(R_{\rm g},0)}, \qquad (3.77)$$

$$T_r = \frac{2\pi}{\kappa} \quad ; \quad T_\psi = \frac{2\pi}{\Omega}.$$

$$\kappa^2(R_{\rm g}) = \left(R\frac{{\rm d}\Omega^2}{{\rm d}R} + 4\Omega^2\right)_{R_{\rm g}}.$$

$$\Omega \lesssim \kappa \lesssim 2\Omega.$$

$$\frac{\kappa_0}{\Omega_0} = 2\sqrt{\frac{-B}{A-B}} = 1.35 \pm 0.05.$$